AMERICAN JOURNAL OF PHYSICAL ANTHROPOLOGY 134:529–534 (2007)

Brief Communication: New Reconstruction of the Taung Endocast

Dean Falk[1]* and Ron Clarke[2]

[1]*Department of Anthropology, Florida State University, Tallahassee, FL 32306-7772*
[2]*Department of Anatomical Sciences, University of the Witwatersrand Medical School, Parktown 2193, Johannesburg, South Africa*

KEY WORDS Taung; virtual endocast; *Australopithecus africanus*; temporal pole; O/M sinus

ABSTRACT Earlier reconstructions of the Taung endocast, from the juvenile type specimen for *Australopithecus africanus*, were achieved without benefit of the advanced computer technology that is available today and before morphological differences were identified that distinguish endocasts of *Paranthropus* from those of *A. africanus*. Here, we reconstruct and measure a relatively complete virtual endocast of Taung and provide a new cranial capacity estimate of 382 cm^3 and a projected adult capacity of 406 cm^3, which are smaller than previous estimates. Linear measurements and ratios were also obtained from an endocast of Sts 5 and five *Paranthropus* endocasts and compared with those of Taung. A number of previously unrecognized foramina, processes, and canals are identified in the bony material that adheres to the base of the Taung endocast. The newly reconstructed virtual endocast of Taung displays a number of shape features that sort it more closely with gracile than robust australopithecines, including squared-off frontal lobes in dorsal view, and the shape of the tips of its temporal poles. The Taung endocast also shares some features with *Paranthropus* endocasts, while other characteristics such as small temporal lobes may be due to its juvenile status. Just how much of Taung's unique morphology is due to its juvenile status may eventually be clarified by comparing its endocast with those from other juvenile australopithecines such as the 3.3-million-year-old juvenile from Dikika, Ethiopia. Am J Phys Anthropol 134:529–534, 2007.

The Taung skull (*Australopithecus africanus*) consists of a natural endocast that reproduced external morphology from the right hemisphere of the brain, a separate portion that contains the face and articulates with the endocast (Dart, 1925), and a mandible that occludes with the maxillary dentition contained in the facial portion. The frontal and right temporal poles are separated from the endocast and embedded in the back of the facial fragment (Schepers, 1946, 1950). Taung manifests several *Paranthropus*-like traits including a sixth cusp on its mandibular first molars (Wood and Abbott, 1983), the shape of its maxillary first molars (Wood and Engleman, 1988), an intrapalatal extension of the maxillary sinus (Conroy and Vannier, 1987), and an enlarged occipital/marginal (O/M) venous sinus on the endocast (Tobias and Falk, 1988; Falk et al., 1995; Falk, 2008). Certain shape features that distinguish the frontal and temporal lobes of *Australopithecus africanus* and *Paranthropus* (Falk et al., 2000) were not known during earlier reconstructions of the Taung endocast (Schepers, 1946; Holloway, 1970), nor had advances in computerized imaging technology yet become available for removing much of the guesswork from mirror imaging, reconstructing, and measuring virtual endocasts (Falk, 2004).

The use of computerized imaging has been validated for visualizing and analyzing endocasts in ways never possible before (Conroy and Vannier, 1985, Tobias 2000), and permits electronic measurement of virtual endocasts from different angles while maintaining their orientation within a particular plane, which is extremely difficult to do by hand. Projected measurements (as opposed to chords) are easily and accurately obtained electronically, but devilishly tricky to do by hand. Electronic measurements are highly repeatable (Falk et al., 2005, 2008). For these reasons, electronic analyses of virtual endocasts are often preferable to those that rely on measurements taken by more traditional methods (see Tobias, 2000; Falk, 2004 for details). Later, we apply these techniques to provide a new virtual reconstruction and cranial capacity estimate, 14 linear measurements, and 20 ratios for the Taung endocast. These data are compared with those from one other *A. africanus* endocast (Sts 5) and five *Paranthropus* endocasts (WT 17000, OH 5, SK 1585, ER 23000, and WT 17400). We also identify foramina and other features on the bony fragments that adhere to the base of the Taung endocast.

MATERIALS AND METHODS

RC reconstructed the right temporal pole of the Taung endocast by applying wet plaster of Paris to the impression (very lightly greased) of its tip that is embedded in the back of the original face. A good quality epoxy cast of the endocast was then quickly locked into position against the back of the facial portion and firmly bound until the plaster had set. When the endocast was then removed, it had a perfect plaster replica of the tip of the temporal lobe in its correct position (Fig. 1). The endocast was then sent to the first author (DF), who identi-

*Correspondence to: Dean Falk, Department of Anthropology, Florida State University, 1847 West Tennessee St., Tallahassee, FL 32306-7772. E-mail: dfalk@fsu.edu

Received 19 February 2007; accepted 20 July 2007

DOI 10.1002/ajpa.20697
Published online 4 September 2007 in Wiley InterScience (www.interscience.wiley.com).

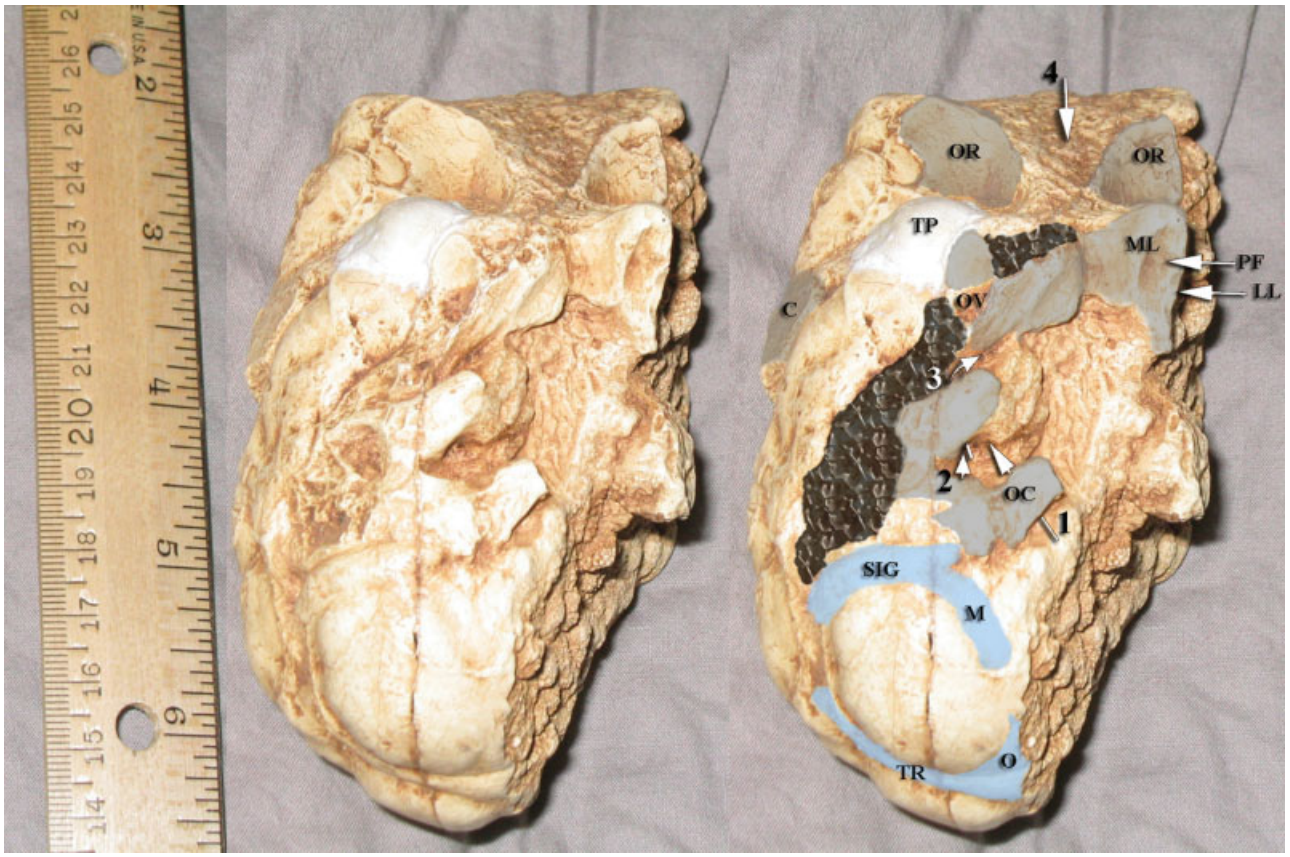

Fig. 1. Cast of the Taung natural endocast shown in basal view with the frontal lobes at the top. The endocast consists mostly of the right hemisphere and is shown here unreconstructed except for the newly-attached tip of the temporal lobe (TP). The image on the right is a key for identifying the morphology that is reproduced on the specimen in the unlabeled image on the left. The endocast has bony fragments (gray) and matrix (black) adhering to it. The larger posterior portion of matrix probably contains internal parts of the petrous temporal bone, since it fills the cleft that is ordinarily created on endocasts by that bone. The left pterygoid fossa and laminae are slightly misaligned relative to the maxillary dentition (not seen here) due to postmortem distortion. Abbreviations: C, chip of bone that adheres to the lateral surface of the right hemisphere; LL, lateral lamina of pterygoid process; ML, medial lamina of pterygoid process; M, marginal sinus; O, occipital sinus; OC, fragment of right occipital condyle; OR, bony orbital plate; OV, foramen ovale in chip of bone; PF, pterygoid fossa, SIG, sigmoid sinus; TR, transverse sinus. Arrows: 1, hypoglossal canal; 2, jugular foramen; 3, carotid canal; 4, triangular area of truncated frontal lobes (the remainder of which are embedded in the facial fragment). [Color figure can be viewed in the online issue, which is available at www.interscience.wiley.com.]

fied previously unrecognized bony features that adhere to its base (Fig. 1).

The endocast with its newly attached temporal pole was scanned with a Konica Minolta Vivid Model no. 910 noncontact 3D digitizer. The digitizing process captured 3D data from all surfaces of the endocast using multiple scans rotated at 30° intervals. Using commercially available software (Raindrop Geomagic, Research Triangle Park, NC), the data were processed, visualized, and inspected for artifacts and damaged areas. The software increased tension on the clear midline that courses along the endocast's dorsal surface and continues ventrally midway between the orbits and medial to the fragment of the left pterygoid process that adheres to the endocast's ventral surface, creating a smooth midline along which the right hemisphere was electronically mirrored. A gap was left in the mirrored endocast at the surface of the midline in the cerebellar regions, and a 3D hard copy of this bilateral endocast was produced using a high-definition 3D printer (Z-corp Spectrum Z-510). DF then used modeling clay to reconstruct the medial portions of the cerebellum and medulla to the level of the foramen magnum in the gap of the hard copy, using the mirrored bony fragment of the occipital condyle and trace of the right marginal sinus (Tobias and Falk, 1988) as guidelines.

The back of the facial fragment contains a roughly triangular area where the frontal poles are embedded that matches the shape of the truncation of the frontal lobes on the endocast. DF carved the polar region out of the back of a slightly damp plaster copy of a Wenner-Gren cast of the facial fragment using the triangular patch, the orbital plates lateral to it, the superior borders of the front part of the orbits in the face, and the contours and thickness of the frontal bone as guides. (Several models were referred during the carving process, including an endocast and cast of the interior of the Skull of Sts 5, an endocast and the interior of a cast of the skull of WT 17400, and an endocast and stereolithographic model of the skull of Sts 71.) The carved shell of the frontal poles was then cast and the resulting partial endocast affixed to the remodeled solid copy of the mirrored endocast, matching the triangular outlines of the two pieces. This composite specimen was scanned with the Konica Minolta no. 910 digitizer, and the data were processed and analyzed electronically (using Geomagic) in order to

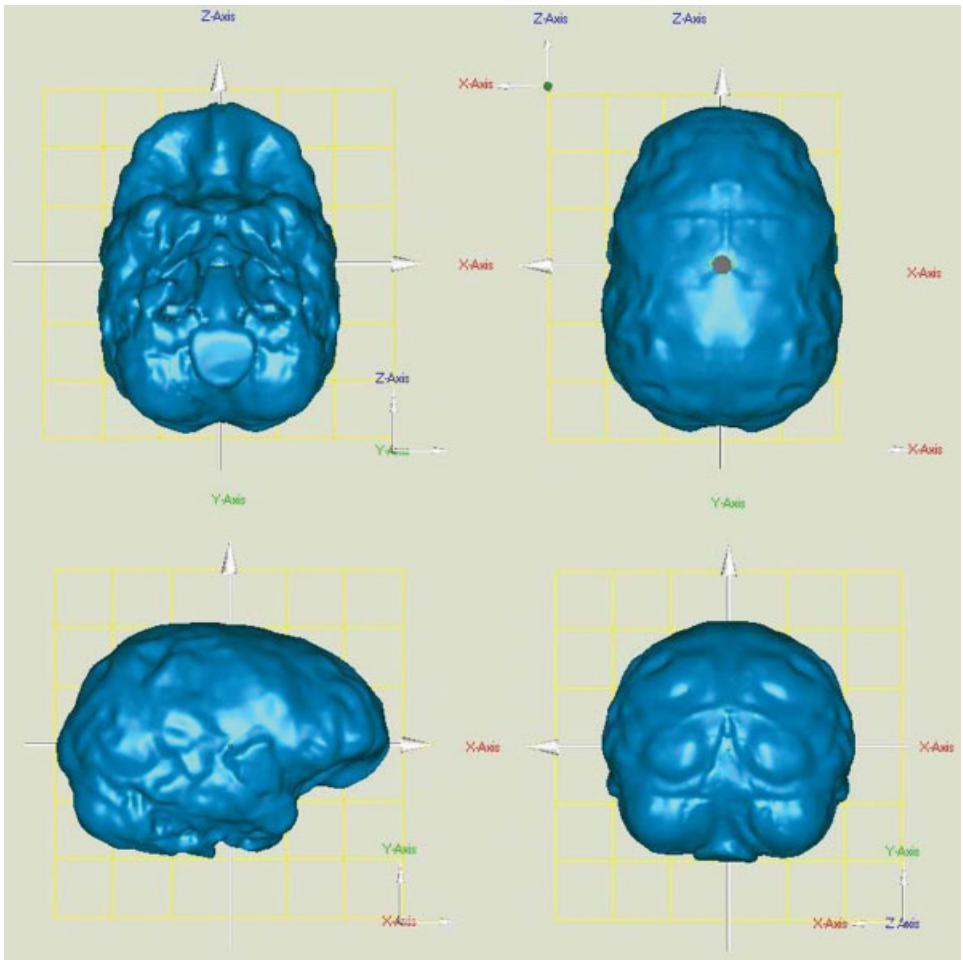

Fig. 2. Clockwise from top-left: basal, dorsal, occipital, and right lateral view of the Taung's virtual endocast aligned with the frontal pole and occipital poles on the horizontal axis. The volume of the endocast as pictured (with adhering matrix and bony fragments) is 399 cm^3; electronic removal of this material yields a volume of 382 cm^3. [Color figure can be viewed in the online issue, which is available at www.interscience.wiley.com.]

register the electronic images of the newly reconstructed basal and frontal regions to the initial electronic version of the mirrored endocast. A hard copy of this final endocast was produced using the high-definition 3D printer.

The volume of the virtual endocast with its adhering matrix and bony fragments was electronically determined to be 399 cm^3 (Fig. 2). Electronic removal of the matrix that filled the cleft created by the petrous portion of the temporal bone and the bony fragments that adhere to the inferior and lateral surfaces of the natural endocast (Fig. 1) yielded a corrected volume for the virtual endocast of 382 cm^3. The matrix between the temporal poles (near sella turcica) was not completely removed because there were no obvious landmarks to guide the process. This excess was balanced to some extent by leaving the slight erosion on the lateral surface of the endocast uncorrected. The 382 cm^3 estimate is consistent with independent corrections obtained by reproducing the visible portions of the matrix and bony fragments in modeling clay, determining their volume by water displacement, and subtracting the value from 399 cm^3.

Fourteen linear measurements that have traditionally been used to describe australopithecine endocasts (Schepers, 1946, 1950; Tobias, 1967; Falk et al., 2000) were obtained electronically from the completed endocast on three occasions, averaged to obtain the final measurements, and ratios computed from these means (Fig. 3 and Table 1). These measurements were highly consistent with an average measurement error across all of the means of less than 1%. The mean measurements were also checked by independently measuring a hard copy of the endocast with calipers. Twenty ratios were computed from the 14 measurements (Table 1). For comparative purposes, the Sts 5 endocast from DF's collection was imaged and measured electronically using the same procedures that were applied to Taung. Ratios were also computed from measurements collected with calipers from *Paranthropus* endocasts in DF's collection (WT 17000, OH5, SK 1585, ER 23000, and WT 17400) (Table 1).

RESULTS

Ratios 1–10 (Table 1) pertain to overall endocast shape. Our measurements for cerebral length and width are shorter than previous estimates, which causes a number of our observations to differ from earlier reports (Schepers, 1946, 1950). Taung's width/length ratio is somewhat smaller than Sts 5's (ratio 1), rather than being exceptionally dolichencephalic as initially described (Schepers, 1946). Taung and Sts 5 are, however,

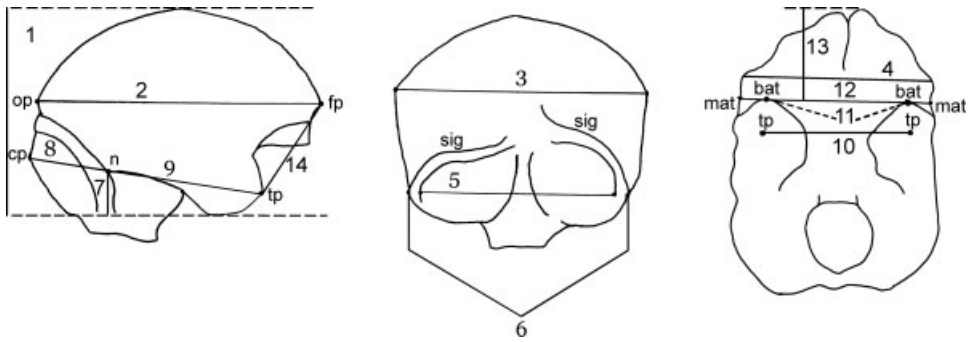

Fig. 3. Key to linear measurements 1–14 in Table 1; right lateral, occipital, and basal views. Landmarks: bat, most anterior point on temporal lobe from basal view; cp, cerebellar pole; fp, frontal pole; mat, most lateral point on endocast at level of bat; n, cerebello-temporal notch; op, occipital pole; tp, temporal pole. For comparative purposes, unilateral measurements were obtained from right hemispheres.

TABLE 1. Endocast measurements (mm) and ratios

		Taung	Sts5	WT 17K	OH 5	SK 1585	ER 23000	WT 17400
1	Endocast hgt	78.5	79.1	74	82	83		
2	lgth	116.0	122.0	116	126		122	
3	wdth	85.5	93.0	91	103	96	100	100
4	fro wdth	75.4	83.0	74				63
5	cbell wdth	66.8	73.8	78	85	74	81	
6	cbell wdth w/sigs	70.7	81.3	83	90	82	89	
7	cbell hgt	21.8	25.3		22	23		
8	cp–tp	75.2	78.7	79	93	78		
9	notch-tp	56.4	64.4	60	68	62		
10	tp–tp	42.9	56.6	54				44
11	bat–bat	44.4	55.4	50				45
12	mat–mat	73.0	83.4	74				68
13	base fro	34.0	35.7	34				29
14	tp-Fp	50.6	54.4	48	50			34
	Volume (cc)	382	473	410	500	476	491	390
	Volume reference	This paper	This paper	Walker et al. (1986)	Falk et al. (2000)	Falk et al. (2000)	Brown et al. (1993)	Holloway (1988b)
1	wdth/lgth	0.74	0.76	0.78	0.82		0.82	
2	hgt/lgth	0.68	0.65	0.64	0.65			
3	hgt/wdth	0.92	0.85	0.81	0.80	0.86		
4	cbell hgt/hgt	0.28	0.32		0.27	0.28		
5	cbell wdth/wdth	0.78	0.79	0.86	0.83	0.77	0.81	
6	cbell wdth/lgth	0.58	0.61	0.67	0.67		0.66	
7	cbell wdth sigs/lgth	0.61	0.67	0.72	0.71		0.73	
8	cbell wdth /fro wdth	0.89	0.89	1.05				
9	fro wdth/lgth	0.65	0.68	0.64				
10	fro wdth/wdth	0.88	0.89	0.81				0.63
11	cp–tp/lgth	0.65	0.65	0.68	0.74			
12	notch-tp/lgth	0.49	0.53	0.52				
13	notch-tp/cp-tp	0.75	0.82	0.76		0.79		
14	tp–tp/lgth	0.37	0.46	0.47				
15	tp–tp/hgt	0.55	0.72	0.73				
16	tp–tp/wdth	0.50	0.61	0.59				0.44
17	tp–tp/fro wdth	0.57	0.68	0.73				0.70
18	bat–bat/mat–mat	0.61	0.66	0.68				0.66
19	bat–bat/base fro	1.31	1.55	1.47				1.55
20	tp–tp/tp–Fp	0.85	1.04	1.13				1.29

base fro, length of rostral frontal lobe in basal view; bat, most anterior point on temporal lobe from basal view; cbell, cerebellum; cp, cerebellar pole; Fp, frontal pole; fro, frontal; mat, most lateral point on endocast at level of bat; notch, cerebello-temporal notch; tp, tip of temporal pole.

Taung and Sts 5 belong to *Australopithecus africanus*, the other specimens are *Paranthropus*. Measurements for Taung and Sts 5 were obtained electronically; the others were collected with calipers. Original references are provided for the listed endocast volumes. The 20 ratios were computed from the 14 linear measurements.

more dolichencephalic than *Paranthropus* endocasts that, conversely, are wider relative to length (Ratio 1), especially at their caudal ends (Ratios 6, 7). *Paranthropus* endocasts also have a relatively narrow frontal width compared with maximum width (ratio 10). These findings are consistent with the signature teardrop shape of robust australopithecine endocasts in dorsal view (Falk et al., 2000). Despite having a *Paranthropus*-like enlarged O/M sinus caudally (Tobias and Falk, 1988), the dorsal outline of the Taung endocast is not

teardrop shaped (Fig. 2). Instead, it resembles the outlines of Sts 5, Sterkfontein No. 2, Sts 60, and Stw 505, which are relatively squared-off at the rostral ends of their frontal lobes (Falk et al., 2000).

Our reconstruction of Taung permits precise measurements involving the temporal poles (Table 1, Ratios 11–20). Length of the back part of the endocast is approximated by the distance between the cerebellar and temporal poles (cp–tp), which is relatively longer compared with endocast length in robust than in gracile australopithecines (Ratio 11), consistent with the elongated frontal lobes of the latter in orbital view (Falk et al., 2000). However, the distance between the cerebello-temporal notch and the tip of the temporal pole (a proxy for temporal lobe length) is absolutely and relatively shorter in Taung than in the other australopithecines (Ratios 12 and 13), which probably reflects its juvenile status (Schepers, 1946).

Taung's immaturity may also account for the absolutely and relatively short distance between the tips of its temporal poles (tp–tp) compared with Sts 5 and WT 17000 (Ratios 14–20), as suggested by Schepers' observation that "Taung's temporal pole is deflected markedly medially at its tip" (Schepers, 1946). Despite the fact that WT 17400 has a recently erupted third molar, its tp–tp measurement is only about 1 mm wider than Taung's. Nevertheless, tp–tp of WT 17400 is much smaller relative to maximum endocast width (Ratio 16) than Taung's, Sts 5's, or WT 17000's. The reverse is true for tp–tp relative to the distance between the right temporal and frontal poles (Ratio 20) because the frontal lobes of WT 17400 are extremely foreshortened (also reflected in Ratio 19). It is also important to note that the tips of Taung's temporal poles appear pointed like those of Sts 5 and less rounded and blunt like those of WT 17000, SK 1585, and WT 17400 (Fig. 2), which is one of the characteristics that distinguishes gracile from robust australopithecines (Falk et al., 2000).

Endocast volumes of 382 and 473 cm^3 were obtained electronically for Taung (after electronically removing adhering matrix and bony fragments) and Sts 5, respectively. Taung's capacity is 23 cm^3 smaller than the ~405 cm^3 estimate (Holloway, 1970) that was published before virtual imaging technology became available for reconstructing endocasts (Falk, 2004). Taung's cranial volume, uncorrected for age, of 382 cm^3 is nearly equal to the estimate for WT 17400 and only 28 mm below that for WT 17000 (Table 1). The endocast differences noted earlier between Taung and these two robust australopithecines are therefore unlikely to be due to allometric scaling. An adult estimate for Taung's cranial capacity was obtained from the ratio between the mean cranial capacity for chimpanzees that (like Taung) have "milk dentition with the first permanent molars erupting or erupted" (365 cm^3) and the mean cranial capacity for adult chimpanzees "with all permanent teeth fully erupted" (390 cm^3), which equals 0.94 (Ashton and Spence, 1958). Thus, Taung's juvenile capacity of 382 cm^3 is 94% of 406 cm^3, which is our new adult estimate and is ~92% of an earlier adult estimate of 440 cm^3 (Holloway, 1970).

DISCUSSION AND CONCLUSIONS

Although identifying precise midlines of endocasts is notoriously difficult because of torques associated with asymmetries in brain shape, current imaging technology has allowed us to mirror image the right hemisphere of the Taung natural endocast with greater precision than can be achieved by hand. Additionally, Taung's temporal and frontal poles were reconstructed from information buried in the back of its facial fragment and incorporated into our new reconstruction. The end result is a virtual endocast from which numerous electronic measurements have been collected. Measurements of virtual endocasts are extremely accurate and reproducible, partly because virtual objects may be fixed within a framework that maintains their relative orientation when they are rotated to obtain measurements from different views. For example, one may flip a virtual endocast in order to take measurements from its basal surface and be assured that the specimen's frontal and occipital poles continue to remain in the same horizontal plane (a widely-used convention for measuring endocasts). Maintaining such orientations is more difficult when measuring endocasts from different views by hand.

A number of previously unrecognized foramina, bony canals, and bony fragments have been identified in the bony material that adheres to the base of the endocast. These include medial and lateral lamina of the left pterygoid fossa, parts of the bony orbits on both sides, a fragment of the right occipital condyle (the one bony feature on the base of the endocast that Dart (1925) apparently recognized and identified as "a portion of the right exoccipital"), the exterior of the right foramen ovale and (on the right) bony remnants of the hypoglossal canal, jugular foramen, and carotid canal (Fig. 1). Some of these identifications were apparent because of their proximity to the marginal portion of Taung's enlarged O/M venous sinus (Tobias and Falk, 1988). Hopefully, the identification of these bony features will be of use to workers seeking data related to the position of the foramen magnum (or other traits) on the base of the skull.

As noted, our electronic measurement of 382 cm^3 for the volume of Taung's endocast is lower than previous measurements, and our estimated adult capacity of 406 cm^3 is 34 cm^3 (~8%) smaller than an earlier estimate of 440 cm^3 (Holloway, 1970). However, the capacity of 473 cm^3 that we obtained electronically for Sts 5 is only 12 cm^3 smaller than the previously published estimate of 485 cm^3 that was determined by water-displacing the endocast (Holloway, 1988a), probably because this endocast required almost no reconstruction. The mean cranial capacity for the five robust australopithecines that we studied is 453 cm^3, while the mean adult capacity for Taung and Sts 5 is slightly smaller (440 cm^3), consistent with an earlier finding that the average cranial capacities for gracile and robust australopithecines appear to be similar (Falk et al., 2000).

Despite this observation, a number of Taung's endocast shape ratios (1, 6, 7, 8, 10, 11) sort it more closely with Sts 5 than robust australopithecines. So do its squared-off frontal lobes in dorsal view and the shape of the tips of its temporal poles (Fig. 2). Other ratios (4, 9, 12, 13, 16) align Taung more closely with *Paranthropus*, although several of these entail small temporal lobes that may be due to Taung's juvenile status. Another *Paranthropus*-like trait of Taung is an enlarged right O/M sinus (Tobias and Falk, 1988), which appears in all 12 scorable robust australopithecines but not in the other five scorable gracile australopithecines (Tobias and Falk, 1988; Falk et al., 1995; Falk, 2008).

The Taung endocast also has unique attributes. As Schepers (1946) observed, its dome appears relatively higher than those of other australopithecines (Ratios 2 and 3). Additionally, Taung is set apart by the relatively

small size of its temporal lobes (ratios 12, 14, 15, 17, 18, 19, 20), consistent with Schepers' suggestion that its "adult temporal lobe would probably have been very extensively expanded, being one of the last cerebral regions to mature during postnatal growth" (Schepers, 1946). The temporal lobe also appears to have been a late bloomer during hominoid evolution, since it is relatively large in humans compared with apes and its components scale allometrically above values predicted from ape regressions (Semendeferi and Damasio, 2000; Rilling and Seligman, 2002). Just how much of Taung's unique morphology is due to its juvenile status may eventually be clarified by comparing its endocast with those from other juvenile australopithecines such as the 3.3-million-year-old juvenile from Dikika, Ethiopia (Alemseged et al., 2006).

ACKNOWLEDGMENTS

We thank Shanon Wooden, Chris Ellis, and Alvin Lim of Florida State University for technical assistance in scanning and analyzing virtual endocasts. Colette Berbesque is thanked for help with casting and Marianne Sarkis for assistance with manuscript preparation.

LITERATURE CITED

Alemseged Z, Spoor F, Kimbel WH, Bobe R, Geraads D, Reed D, Wynn JG. 2006. A juvenile early hominin skeleton from Dikika, Ethiopia. Nature 443:296–301.

Ashton EH, Spence TF. 1958. Age changes in the cranial capacity and foramen magnum of hominoids. Proc Zool Soc Lond 130:169–181.

Brown B, Walker A, Ward CV, Leakey RE. 1993. New *Australopithecus boisei* calvaria from east Lake Turkana. Am J Phys Anthropol 91:137–159.

Conroy GC, Vannier MW. 1985. Endocranial volume determination of matrix-filled fossil skulls using high-resolution computed tomography. In: Tobias PV, editor. Hominid evolution: past, present and future. New York: Alan R. Liss, p 419–426.

Conroy GC, Vannier MW. 1987. Dental development of the Taung skull from computerized tomography. Nature 329:625–627.

Dart RA. 1925. *Australopithecus africanus*: the man-ape of South Africa. Nature 115:195–199.

Falk D. 2004. Hominid brain evolution—new century, new directions. Coll Antropol 28:59–65.

Falk D. 2008. Brain evolution: the radiator hypothesis. In: Squire LR, editor. New encyclopedia of neuroscience. Oxford: Elsevier, in press.

Falk D, Gage TB, Dudek B, Olson TR. 1995. Did more than one species of hominid coexist before 3.0 Ma? Evidence from blood and teeth. J Hum Evol 29:591–600.

Falk D, Hildebolt C, Smith K, Morwood MJ, Sutikna T, Brown P, Jatmiko, Saptomo EW, Brunsden B, Prior F. 2005. The brain of LB1, *Homo floresiensis*. Science 308:242–245.

Falk D, Hildebolt C, Smith K, Morwood MJ, Sutikna T, Jatmiko, Saptomo EW, Inhof H, Seidler H, Prior F. 2007. Brain shape in human microcephalics and *Homo floresiensis*, Proc Natl Acad Sci USA 104:2513–2518.

Falk D, Redmond JC Jr, Guyer J, Conroy GC, Recheis W, Weber GW, Seidler H. 2000. Early hominid brain evolution: a new look at old endocasts. J Hum Evol 38:695–717.

Holloway RL. 1970. Australopithecine endocast (Taung specimen, 1924): a new volume determination. Nature 168:966–968.

Holloway RL. 1988a. Brain. In: Tattersall I, Delson E, van Covering J, editors. Encyclopedia of human evolution and prehistory. New York: Garland. p 98–105.

Holloway RL. 1988b. "Robust" australopithecine brain endocasts: some preliminary observations. In: Grine F, editor. Evolutionary history of the "Robust" Australopithecines. New York: Aldine de Gruyter. p 97–105.

Rilling JK, Seligman RA. 2002. A quantitative morphometric comparative analysis of the primate temporal lobe. J Hum Evol 42:505–533.

Schepers GWH. 1946. The endocranial casts of South African Ape-men. Transvaal Mus Mem 2:155–272.

Schepers GWH. 1950. The brain casts of recently discovered *Plesianthropus* skulls. Transvaal Mus Mem 4:85–117.

Semendeferi K, Damasio H. 2000. The brain and its main anatomical subdivisions in living hominoids using magnetic resonance imaging. J Hum Evol 38:317–332.

Tobias PV. 1967. Olduvai Gorge. The cranium and maxillary dentition of Australopithecus (Zinjanthropus) boisei, Vol. 2. Cambridge: Cambridge University Press.

Tobias PV. 2000. The promise and the peril in hominin brain evolution. In Falk D, Gibson KR, editors. Evolutionary anatomy of the primate cerebral cortex. Cambridge: Cambridge University Press. p 241–256.

Tobias PV, Falk D. 1988. Evidence for a dual pattern of cranial venous sinuses on the endocrainal cast of Taung (*Australopithecus africanus*). Am J Phys Anthropol 76:309–312.

Walker AC, Leakey RE, Harris JM, Brown RH. 1986. 2.5-Myr *Australopithecus boisei* from west of Lake Turnkana, Kenya. Nature 322:517–522.

Wood BA, Abbott SA. 1983. Analysis of dental morphology of the Plio-pleistocene hominids. I. Mandibular molars: crown area measurements and morphological traits. J Anat 136:197–219.

Wood BA, Engleman CA. 1988. Analysis of the dental morphology of Plio-pleistocene hominids. V. Maxillary postcanine tooth morphology. J Anat 161:1–35.